BIOLOGY OF REPRODUCTION (2014) **91**(3):74, 1–15
Published online before print 6 August 2014.
DOI 10.1095/biolreprod.114.118562

FSH Receptor (FSHR) Expression in Human Extragonadal Reproductive Tissues and the Developing Placenta, and the Impact of Its Deletion on Pregnancy in Mice[1]

Julie A.W. Stilley,[3] Debora E. Christensen,[3] Kristin B. Dahlem,[3] Rongbin Guan,[3] Donna A. Santillan,[4] Sarah K. England,[5] Ayman Al-Hendy,[6] Patricia A. Kirby,[7] and Deborah L. Segaloff[2,3]

[3]*Department of Molecular Biophysics and Physiology, University of Iowa Roy J. and Lucille A. Carver College of Medicine, Iowa City, Iowa*
[4]*Department of Obstetrics and Gynecology, University of Iowa Roy J. and Lucille A. Carver College of Medicine, Iowa City, Iowa*
[5]*Department of Obstetrics and Gynecology, Washington University School of Medicine, St. Louis, Missouri*
[6]*Department of Obstetrics and Gynecology, Meharry Medical Center, Nashville, Tennessee*
[7]*Department of Pathology, University of Iowa Roy J. and Lucille A. Carver College of Medicine, Iowa City, Iowa*

ABSTRACT

Expression and function of the follicle-stimulating hormone receptor (FSHR) in females were long thought to be limited to the ovary. Here, however, we identify extragonadal FSHR in both the human female reproductive tract and the placenta, and test its physiological relevance in mice. We show that in nonpregnant women FSHR is present on: endothelial cells of blood vessels in the endometrium, myometrium, and cervix; endometrial glands of the proliferative and secretory endometrium; cervical glands and the cervical stroma; and (at low levels) stromal cells and muscle fibers of the myometrium. In pregnant women, placental FSHR was detected as early as 8–10 wk of gestation and continued through term. It was expressed on: endothelial cells in fetal portions of the placenta and the umbilical cord; epithelial cells of the amnion; decidualized cells surrounding the maternal arteries in the maternal decidua; and the stromal cells and muscle fibers of the myometrium, with particularly strong expression at term. These findings suggest that FSHR expression is upregulated during decidualization and upregulated in myometrium as a function of pregnancy. The presence of FSHR in the placental vasculature suggests a role in placental angiogenesis. Analysis of genetically modified mice in which *Fshr* is lacking in fetal portions of the placenta revealed adverse effects on fetoplacental development. Our data further demonstrate *FSHB* and *CGA* mRNAs in placenta and uterus, consistent with potential local sources of FSH. Collectively, our data suggest heretofore unappreciated roles of extragonadal FSHR in female reproductive physiology.

cervix, follicle-stimulating hormone, FSH receptor, gonadotropin, placenta, pregnancy, uterus

INTRODUCTION

The field of female reproductive physiology has traditionally considered follicle-stimulating hormone receptor (FSHR) expression and function to be limited to the ovary, where FSH signaling stimulates follicular growth and estrogen synthesis. However, recent studies suggest that FSHR is also present in extragonadal tissues, including some that are unrelated to reproduction. Examples of the latter include osteoclasts, where FSH signaling mediates bone resorption [1, 2], and endothelial cells of the tumor vasculature, where its role has not yet been elucidated [3].

The following earlier reports are relevant to FSHR expression and function in extragonadal tissues of the female reproductive tract. Bovine cervix was reported to express FSHR (at both the mRNA and protein levels), and FSH was shown to stimulate prostanoid synthesis in this tissue [4]. In the human endometrium, decidualization is associated with an increase in levels of the FSHR mRNA [5]. Studies in the rat myometrium have indicated that FSH affects electrical activity, although they did not address FSHR expression on the protein or mRNA level [6, 7]. Radu et al. [3] reported that endothelial cells in the chorionic villi of the human placenta at term express FSHR. Finally, we have demonstrated that human umbilical vein endothelial cells (HUVECs) express FSHR, and that FSH stimulates the formation of endothelial tubes and other angiogenic processes with an efficacy comparable to that of vascular endothelial growth factor (VEGF) [8]. We also found that FSH did not stimulate VEGF secretion by HUVECs, suggesting that it signals through endothelial FSHR directly to stimulate angiogenesis. Interestingly, the FSHR in HUVECs is a splice variant that lacks exon 9 [8], the same FSHR splice variant that is expressed in osteoclasts [9, 10].

Notably, *FSHR* was identified as a gene involved in the timing of birth in humans in 2011, when Plunkett et al. [11] discovered an association between intronic *FSHR* SNPs and preterm birth. It is difficult to reconcile ovarian FSHR as contributing to the timing of birth; it seems more likely that extragonadal sites of FSHR expression are physiologically relevant in this context.

In light of the many lines of evidence pointing to roles for FSHR outside the ovary, we undertook the present study, systematically and thoroughly examining human extragonadal female reproductive tissues and the placenta for FSHR protein expression. Our data reveal novel patterns of extragonadal FSHR expression that are suggestive of roles for FSHR signaling that were not previously considered. Furthermore, we

[1]These studies were supported in part by National Institutes of Health (NIH) grants HD022196 to D.L.S. and HD037831 to S.K.E. J.A.W.S. was supported by NIH grant T32DK007690, D.E.C. by a University of Iowa Carver College of Medicine FUTURE in Biomedicine Fellowship, and K.B.D. by a Drake University Fellowship.
[2]Correspondence: Deborah L. Segaloff, Department of Molecular Physiology and Biophysics, 5–470 Bowen Science Building, 51 Newton Rd., University of Iowa, Iowa City, IA 52242.
E-mail: deborah-segaloff@uiowa.edu

Received: 13 February 2014.
First decision: 15 April 2014.
Accepted: 21 July 2014.

eISSN: 1529-7268 http://www.biolreprod.org
ISSN: 0006-3363

provide evidence substantiating the physiological relevance of placental endothelial FSHR; genetically modified mice lacking *Fshr* in the fetal component of the placenta undergo abnormal fetoplacental growth.

MATERIALS AND METHODS

Antibodies

FSHR-323 hybridoma cells, which express an immunoglobulin G2a (IgG2a) that recognizes the extracellular domain of the human FSHR and were created and characterized by Radu et al. [3] and Vannier et al. [12], were obtained from the American Type Tissue Collection, ascites was prepared, and purified IgG2a was generated using the NAb protein G Spin Kit (Thermo Fisher Scientific Inc., Waltham, MA). Purified nonimmune mouse IgG2a was obtained from R&D Systems (Minneapolis, MN).

Rabbit anti-rat FSHR was generously provided by Dr. Mario Ascoli (University of Iowa). Its characterization and specificity have been described previously [13]. This antibody, unlike FSHR-323, cross-reacts with mouse FSHR.

Sample Collection of Human Tissues

Slides of deidentified human tissues were obtained from the University of Iowa Hospital and Clinics Department of Pathology. Deidentified samples of placenta and umbilical cord at term pregnancy were also obtained through the Maternal Fetal Tissue Bank (Institutional Review Board [IRB] no. 200910784) of the University of Iowa Hospital and Clinics Department of Obstetrics and Gynecology. All patients signed written consent forms approved by the IRB (no. 200910784). Human myometrial tissue was also obtained from the lower uterine segment from women undergoing elective cesarean delivery under spinal anesthesia at late pregnancy (38–40 wk gestation) and in the absence of spontaneous or induced labor contractions. In the latter case, all patients signed written consent forms approved by the IRB (no. 199809066). Samples were either prepared for histology or stored at −80°C in RNAlater (Qiagen, Valencia, CA) for subsequent RNA isolation.

Immunohistochemistry of Human Tissues

Generally, for each stage and/or tissue type, samples from at least four different patients were examined. The exceptions were placenta at 28–30 wk gestation and cervix, in which cases only two samples were available. Regardless of the tissue examined, no variability in staining patterns across patients was observed. Samples were deparaffinized in xylenes and rehydrated in an ethanol series. Antigen retrieval was performed using citrate buffer at 95°C for 15 min. During immunohistochemistry, nonspecific binding was blocked by incubating the samples with filtered PBS (PBS-IH; 137 mM NaCl, 2.7 mM KCl, 1.4 mM KH_2PO_4, and 4.3 mM Na_2HPO_4 [pH 7.4]) containing 10% normal goat serum (Sigma Aldrich, St. Louis, MO) for 2 h at room temperature. FSHR-323 IgG2a and nonimmune IgG2a were each used at 5 μg/ml and were applied in blocking buffer overnight at 4°C. After washing, biotinylated goat anti-mouse secondary antibody (4.2 μg/ml; Jackson ImmunoResearch Laboratories Inc., West Grove, PA) was added for 1 h at room temperature. The ABC Standard Kit (Vector Laboratories Inc., Burlingame, CA) was used as per the manufacturer's instructions, and immunoreactivity was visualized with 3,3-diaminobenzidine (Dako North America Inc., Carpinteria, CA) developed for 30 sec. Tissues were counterstained by applying 10% Harris hemotoxylin (Leica Microsystems Inc., Buffalo Grove, IL) before dehydration, and then coverslips were applied. Microscopic viewing and interpretation of the slides were performed with a pathologist (P.A.K.). Images were captured using an Olympus BX61 Light Microscope (Center Valley, PA). Nonhuman primate ovary served as a control, with staining carried out as described above. As expected, specific immunostaining of follicular granulosa cells was observed [8].

Staining in myometrial sections was quantified using ImageJ software (National Institutes of Health, Bethesda, MD) according to the manufacturer's instructions, with the following modifications. The analysis was limited to FSHR from myometrial smooth muscle by focusing on rectangles of uniform size at the top, right, bottom, left, and center of each image, shifting these as necessary to tissue to avoid blood vessels. For each rectangle, the percentage of pixels exceeding a threshold value of 160 was determined, and then the percentages for all rectangles on a given slide were averaged.

Immunofluorescence Microscopy

Stably transfected 293 cells expressing recombinant human FSHR or human luteinizing hormone/chorionic gonadotropin receptor (LHR) [14] were plated on glass slides before fixation in 4% paraformaldehyde. Nonspecific binding was blocked by incubation in PBS-IH containing 5% bovine serum albumin. Antibody FSHR-323 IgG2a or nonimmune IgG2a was added at 10 μg/ml in blocking buffer for 1 h at room temperature. After washing, Alexa Fluor goat anti-mouse 568 (4 μg/ml; Invitrogen) was added for 1 h at room temperature before slides were mounted in antifade mounting medium containing 4′,6-diamidino-2-phenylindole. Images were captured on a fluorescence microscope.

PCR Amplification of FSHR mRNA From Human Myometrium

Myometrial tissue stored in RNAlater was minced and homogenized. Total RNA was isolated using the PureLink RNA Mini Kit (Ambion/Life Technologies, Grand Island, NY) per the manufacturer's instructions, with the addition of on-column PureLink DNase treatment. RNA was quantified using a NanoDrop 1000 spectrophotometer (NanoDrop Technologies, Wilmington, DE). Pooled human ovarian RNA was purchased from Clontech (Mountain View, CA).

Reverse transcription was performed with 2 μg of RNA using the SuperScript III First-Strand Synthesis System for RT-PCR (Life Technologies) as described previously [8]. Polymerase chain reactions were performed using Taq DNA Polymerase with Standard Taq Buffer (New England BioLabs, Ipswich, MA) containing magnesium chloride. After 2 min of 95°C, 40 cycles of 95°C, 55°C–59°C (depending on the primers), and 68°C were used in a Bio-Rad iCycler iQ Thermocycler (Hercules, CA).

Oligonucleotide primers were obtained from Integrated DNA Technologies (Coralville, IA). Traditional PCR methods using random hexamers for reverse transcription were used to amplify exons 2–3 of *FSHR* mRNA, as described previously [9, 10]. Primers spanning exons 2–3 of the *FSHR* mRNA (expected size: 120 bp) were: forward, CTCACCAAGCTTCGAGTCATCCAA; and reverse, AAGGTTGGAGAACACATCTGCCTCT. To test for the presence of *FSHR* mRNA splice variants [9, 10, 15], PCR amplifications of exons 8–10, 1–4, or 4–7 of *FSHR* mRNA were performed using a modified, more sensitive procedure [8–10] in which gene-specific reverse transcription reactions were performed using 20 pM reverse primers of each primer set (see below) before PCR. Primers spanning exons 8–10 (expected sizes: 320 bp for *FSHR* mRNA containing exons 8, 9, and 10; and 140 bp for a splice variant lacking exon 9 [Δ9]) were: forward, AGCCTCTGGACCAGTCATTCT; and reverse, CTCTGCTGTAGCTGGACTCAT; as described previously [8–10]. Primers spanning exons 1–4 (expected sizes: 237 bp for *FSHR* mRNA containing exons 1, 2, 3, and 4; and 166 bp for a splice variant lacking exon 2 [Δ2]) were: forward, CTGCCAAGAGAGCAAGGTGA; and reverse, GTAGAG CAGGTTGTTGGCCT. Primers spanning exons 4–7 (expected sizes: 279 bp for *FSHR* mRNA containing exons 4, 5, 6, and 7; and 202 bp for a splice variant lacking exon 6 [Δ6]) were: forward, GCCAACAACCTGCTCTACAT; and reverse, GCTCATCTAGTTGGGTTCCATT. Products were visualized on a 2% agarose gel.

PCR Amplification of mRNAs Encoding FSH Subunits

Amplification of mRNA encoding the β subunit of FSH (*FSHB* mRNA) and the α subunit of the glycoprotein hormones (*CGA* mRNA) was performed using traditional PCR on human pituitary cDNA (Biochain Institute, Newark, CA) or modified PCR using gene-specific reverse transcription (described immediately above) on all other human reproductive tissues tested. Human umbilical vein endothelial cells were obtained and cultured as described previously [8]. Primers for *FSHB* mRNA were those described by Bieche et al. [16]. The primers spanning exons 2–3 of *FSHB* mRNA (expected size: 144 bp) were: forward, TGGTGTGCTGGCTACTGCTAC; and reverse, ATACAAG GAATCTGCATGGTGAG. Primers for the *CGA* mRNA spanning exons 1–3 (expected size: 177 bp) were: forward, GAGAAAGGAGCGCCATGGATTA; and reverse, CAGCCCATGCACTGAAGTATTG.

FORKO Mice

FORKO mice, which represent a global knockout of *Fshr* and were created and characterized by Dr. R. Sairam [17–19], were rederived (A.A.-H.) with Dr. Sairam's permission. These mice were then moved to, and bred at, the University of Iowa Animal Facility. All animals were housed under standard conditions, on a 12L:12D cycle, with access to water and food ad libitum. Animal care procedures were approved by the Institutional Animal Care and

Use Committee for the University of Iowa, and were performed in accordance with the standards set by the National Institutes of Health. At weaning, the mice were separated by sex, and an ear punch was performed for identification and DNA genotyping.

To facilitate the collection of placental and fetal tissues, we synchronized postpubertal $Fshr^{+/-}$ females in the estrous cycle, as described by Whitten [20]. $Fshr^{+/-}$ females thus treated were caged with $Fshr^{+/-}$ males, and pregnant dams were killed 14–16 days post conception (dpc). Uteri were excised and the fetoplacental units were removed. The fetus and placenta were then separated and weighed individually. Fetuses were snap frozen and stored for genotyping. A total of 54 fetoplacental units were isolated from 9 pregnant dams. For each pregnant dam, the weight of each fetus was normalized to the mean weight of the $Fshr^{+/-}$ fetuses in that litter, and the weight of each placenta was normalized to the mean weight of the placentae associated with the $Fshr^{+/-}$ fetuses. (Normalization was not performed relative to $Fshr^{+/+}$ littermates because they were not present in all litters). Therefore, the values for each fetus and placenta were expressed as a percentage of the mean weight for the heterozygotes in that litter. Normalized data for fetuses and placentae from all pregnant dams were then pooled and analyzed.

Genotyping

Frozen ear punches or fetal tissue (approximately 20 mg) were used to genotype the FORKO mice. DNA was extracted using the DNeasy Blood & Tissue Kit as per the manufacturer's instructions (Qiagen). The PCR for *Fshr* genotyping was performed as described previously [17].

Immunohistochemistry of Mouse Tissues

$Fshr^{+/-}$ mice were crossed and term placentae from wild-type and $Fshr^{-/-}$ littermates were collected and stained for FSHR. The protocol was essentially the same as described above for human tissues, except that rabbit anti-rat FSHR (1:5000) or preimmune rabbit serum at the same dilution (negative control) was used as the primary antibody, and biotinylated goat anti-rabbit IgG Fab (1:500) from Jackson ImmunoResearch Laboratories was used as the secondary antibody.

Statistical Analyses

Quantified data are expressed as the mean ± SEM. The statistical significance of differences between groups was determined using the Student *t*-test, or one-way ANOVA where appropriate. Analyses were performed using GraphPad Prism (GraphPad Software Inc., La Jolla, CA). Significance was defined as $P < 0.05$.

RESULTS

Localization of FSHR in the Human Term Placenta and Associated Tissues

Expanding upon previous findings reported by Radu et al. [3] demonstrating FSHR expression in the endothelial cells of blood vessels in the chorionic villi of term human placenta, we sought to determine sites of FSHR expression in placentae from various stages of pregnancy, starting with term placentae. These studies were performed with antibody FSHR-323, a monoclonal antibody against human FSHR [3, 12]. Previous studies by Vannier et al. [12] and Radu et al. [3] had validated the specificity of antibody FSHR-323 by showing, among other criteria, expected patterns of FSHR expression in human ovary and testes. In addition, using antibody FSHR-323, we previously demonstrated the expected FSHR localization when staining nonhuman primate ovary [8]. Herein, we further demonstrate that antibody FSHR-323 stains 293 cells expressing recombinant human FSHR, but not cells expressing recombinant human LHR (Supplemental Fig. S1; Supplemental Data are available online at www.biolreprod.org).

In placentae collected between 38 and 40 wk gestation, FSHR staining was intense in the endothelial cells of blood vessels in the chorionic villi (Fig. 1, A and B). FSHR staining was also visible, albeit less prominent, in the stromal cells of the villi (Fig. 1A). Examination of chorionic villi at higher magnification revealed that trophoblasts did not express FSHR (Fig. 1B). Examination of the amnion-chorion interface indicated that FSHR is expressed in the epithelial cells of the outer layer of the amnion (Fig. 1C), as well as in stromal fibroblasts.

Within the maternal decidua (Fig. 1, C and D), the stroma was found to be positive for FSHR staining. Notably, the staining was quite intense in clustered subsets of decidual cells (labeled D_1 in Fig. 1D), whereas in general the decidual cells within the stroma exhibited more moderate levels of expression (labeled D_2). In addition, endothelial cells of the maternal blood vessels in the decidua stained for FSHR (Fig. 1C). It should be noted that underlying the layer of strongly stained decidua, nonspecific staining of neutrophils was observed (labeled N in Fig. 1D). Because of their high myeloperoxidase content, neutrophils typically exhibit nonspecific staining, regardless of the primary antibody.

Examination of term umbilical cord revealed FSHR expression in the endothelial cells of the umbilical artery, as well as in both the inner and outer layers of the smooth muscle of this structure (Fig. 2A). Within the umbilical vein (Fig. 2B), the tunica interna (endothelial cells) stained strongly and the tunica media moderately (Fig. 2B). Fibroblasts within Wharton jelly also expressed FSHR, as did the amniotic epithelium (Fig. 2C).

Localization of FSHR in Human Placenta and Its Associated Tissues at 28–30 wk Gestation

Analysis of placentae and umbilical cords collected between 28 and 30 wk gestation revealed patterns of FSHR staining similar to those described above for term samples. In the case of the placentae, intense staining for FSHR was observed in endothelial cells of the chorionic villi (Fig. 3A), and this was the case for both small, developing vessels and larger, more mature vessels; more moderate FSHR staining was visible in the stromal cells of the villus, as was most readily seen in the anchoring villi; and no staining was observed in the case of trophoblasts (Fig. 3B). At the amnion-chorion interface, amniotic epithelial cells (Fig. 3B), stromal fibroblasts, maternal decidual cells, and endothelial cells of maternal blood vessels (Fig. 3C) were positive for FSHR. Again, clustered subsets of decidual cells stained intensely for FSHR, whereas others stained weakly, and endothelial cells stained intensely.

Localization of FSHR in Human Placenta and Its Associated Tissues at 18–20 wk Gestation

Analysis of placentae collected between 18 and 20 wk gestation also yielded results similar to those reported above for their more mature counterparts. In spite of the fact that many of the chorionic vessels develop into more mature vessels during this period, FSHR staining was intense in the endothelial cells of chorionic villi (Fig. 4A); this was the case regardless of maturity of the chorionic villi, size of the vessel, or location of the vessel. Moreover, stromal cells were positive, and trophoblasts negative, for FSHR staining.

Results for the amnion-chorion interface were likewise consistent with the findings from later time points. Both the amniotic epithelial layer and the stromal fibroblasts were positive for FSHR staining, with much stronger staining in the epithelial layer (Fig. 4B). Also, in umbilical artery FSHR was expressed in endothelial cells and in the two muscle layers of the arteries (Fig. 4C), and in the umbilical vein it was present in the endothelial tunica interna, the tunica media, and fibroblasts of Wharton jelly (Fig. 4D).

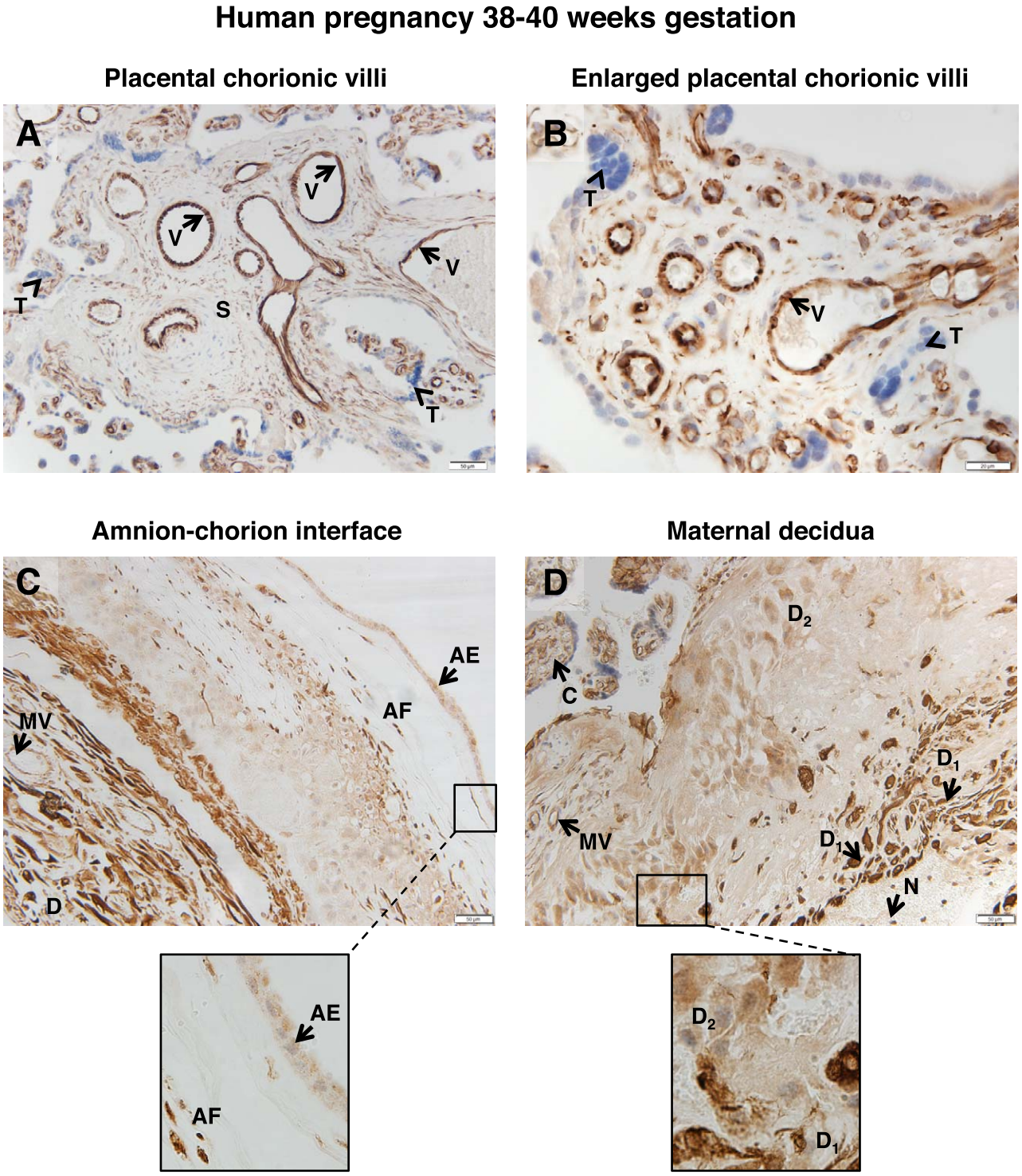

FIG. 1. FSHR expression in human placenta and associated tissues at 38–40 wk gestation. Tissues were stained with antibody FSHR-323 IgG2a (brown) and counterstained with hematoxylin (blue). **A** and **B**) Chorionic villi (magnifications ×200 [**A**] and ×600 [**B**]). Labeled are endothelial cells of the villi vessels (V), the chorionic stromal core (S), and trophoblasts (arrowhead labeled T). **C**) Amnion-chorion interface, including the amnion, chorion, and maternal decidua (magnification ×200; inset ×600). Labeled are the amniotic epithelium (AE), amniotic fibroblasts (AF), maternal decidua (D), and endothelial cells of the maternal vessels (MV). **D**) Maternal decidua (magnification ×200; inset ×600). Labeled are decidua strongly stained for FSHR (D_1), decidua moderately stained for FSHR (D_2), chorionic villi (C), and nonspecific staining of neutrophils (N). Corresponding negative controls stained with nonimmune IgG2a at the same concentration are shown in Supplemental Figure S2.

The maternal decidua at 18–20 wk gestation is of particular interest because at this stage maternal spiral arteries are actively remodeling. As shown in Figure 5A, the expression of FSHR in decidual cells was nonhomogeneous, being strongly expressed in clustered groups of decidual cells, but weakly or not at all in others. Notably, and as is more clearly observed in the higher-magnification views shown in Figure 5, B–D, the inner linings of the maternal vessels were sometimes positive and sometimes negative for FSHR. The absence of FSHR in maternal vessels seems to correlate with vessel remodeling,

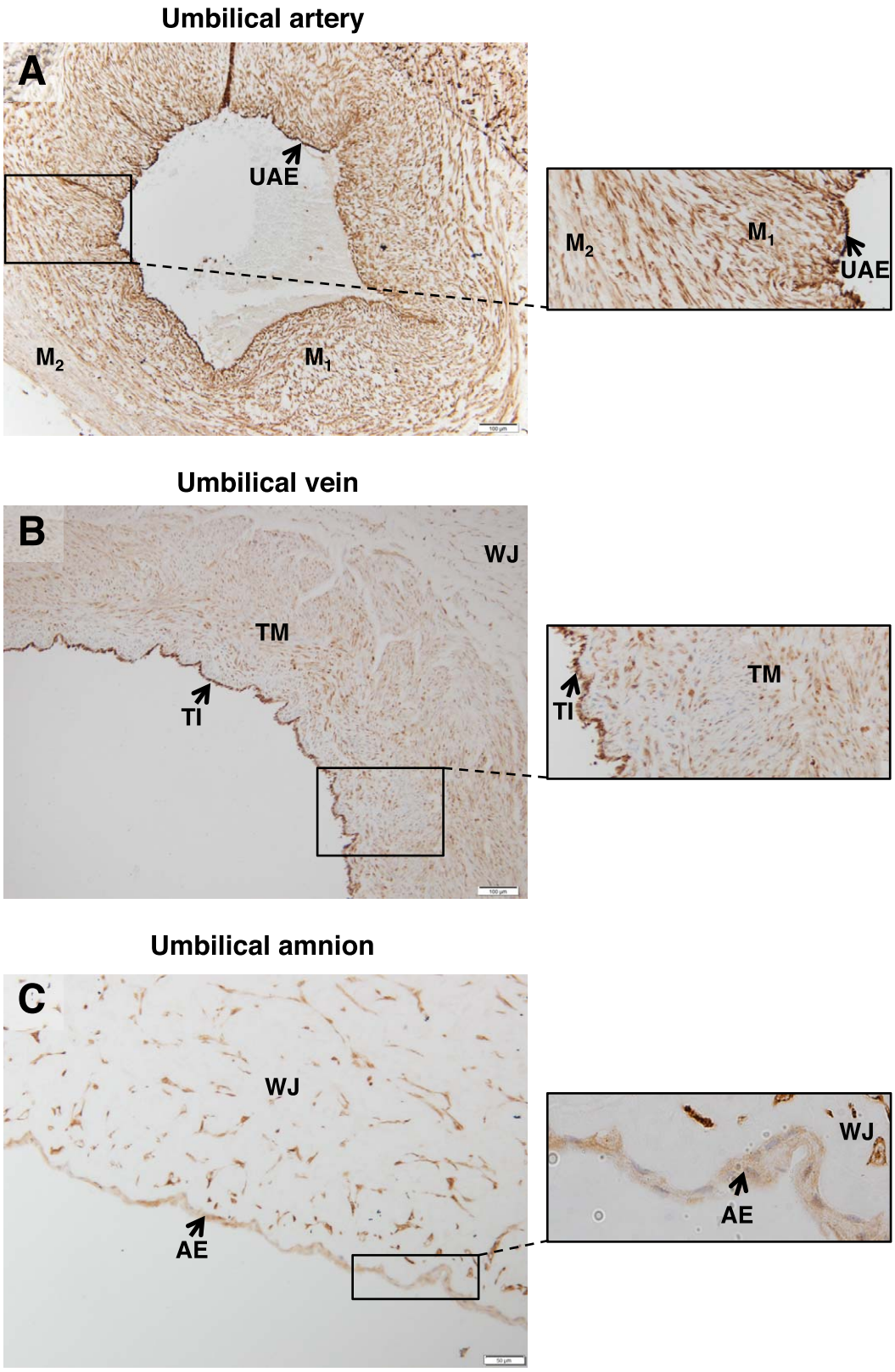

FIG. 2. FSHR expression in human umbilical cord at 38–40 wk gestation. Tissues were stained with antibody FSHR-323 IgG2a (brown) and counterstained with hematoxylin (blue). **A**) Umbilical artery (magnification ×100; inset ×200). Labeled are the endothelium (UAE), the inner layer of smooth muscle (M_1), and the outer layer of smooth muscle (M_2). **B**) Umbilical vein (magnification ×100; inset ×200). Labeled are the tunica intima (TI), tunica media (TM), and Wharton jelly (WJ). **C**) Cord amnion (magnification ×200; inset ×600). Labeled are the amniotic epithelium (AE) and Wharton jelly (WJ). Corresponding negative controls stained with nonimmune IgG2a at the same concentration are shown in Supplemental Figure S3.

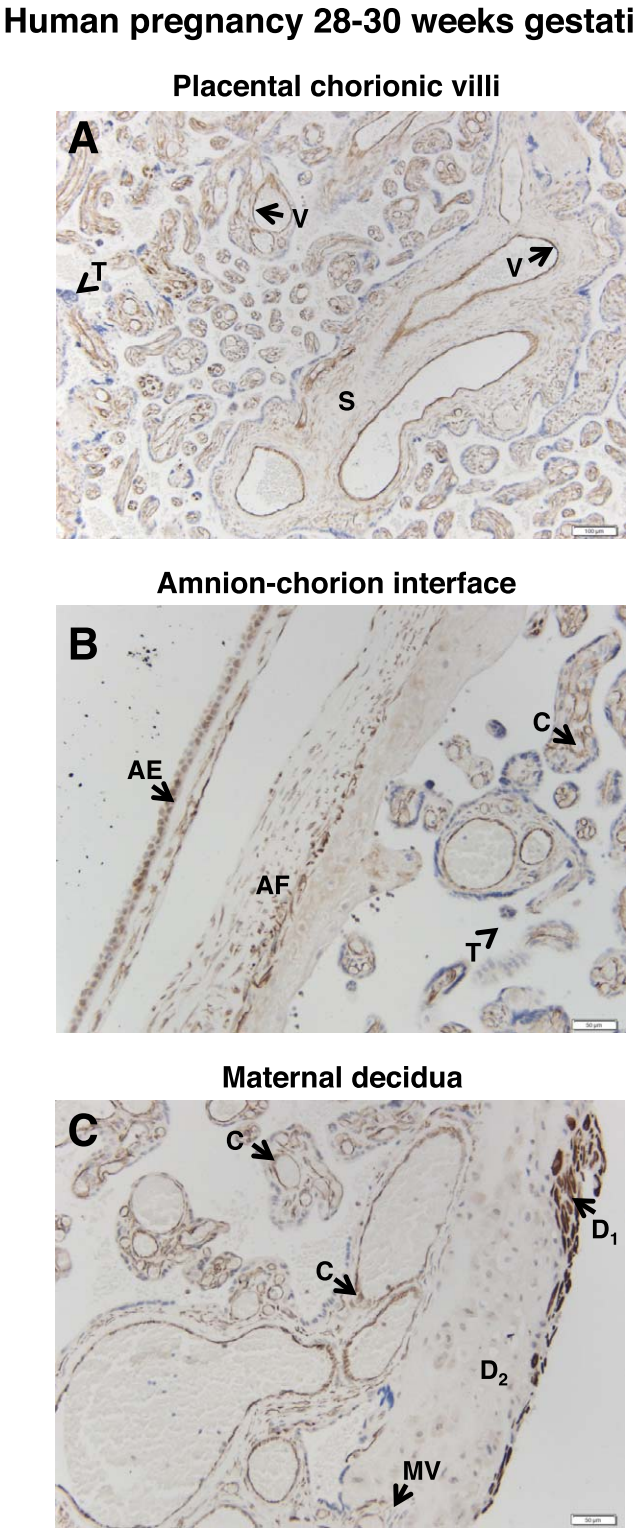

FIG. 3. FSHR expression in human placenta and associated tissues at 28–30 wk gestation. Tissues were stained with antibody FSHR-323 IgG2a (brown) and counterstained with hematoxylin (blue). **A**) Chorionic villi (magnification ×100). Labeled are the endothelial cells of villi vessels (V), the chorionic stromal core (S), and trophoblasts (arrowhead labeled T). **B**) Amnion-chorion interface (magnification ×200). Labeled are the amniotic epithelium (AE), amniotic fibroblasts (AF), chorionic villi (C), and trophoblasts of the chorionic villi (arrowhead labeled T). **C**) Maternal decidua (magnification ×200). Labeled are decidua strongly stained for FSHR (D_1), decidua moderately stained for FSHR (D_2), endothelial cells of the maternal vessels (MV), and chorionic villi (C). Corresponding negative controls stained with nonimmune IgG2a at the same concentration are shown in Supplemental Figure S4.

given the presence of invading extravillous trophoblasts lining maternal vessels and thus lacking endothelial cells in those sections (Fig. 5C and lower rectangle of Fig. 5B). The areas adjacent to maternal vessels lacking FSHR staining were populated with decidual cells staining intensely for FSHR (Fig. 5C and lower rectangle of Fig. 5B). In contrast, in areas of maternal vessels that had not yet undergone remodeling and had endothelial cells still present, FSHR expression was observed in the endothelium, and in this case the nearby decidual cells stained less intensely for FSHR (Fig. 5D and upper rectangle of Fig. 5B).

Localization of FSHR in Human Placenta and Associated Tissues at 8–10 wk Gestation

Interestingly, FSHR expression was detected as early as 8–10 wk gestation, the earliest time frame examined. In placentae collected between 8 and 10 wk gestation, FSHR was again strongly expressed in endothelial cells of the developing chorionic villi (Fig. 6A), moderately expressed in stromal cells of the chorionic vessels, and not expressed in trophoblasts. However, unlike decidua at later stages of gestation, FSHR staining was generally strong through most of the decidua, with the regions adjacent to the chorion and surrounding the maternal lacunae being particularly intense (Fig. 6B). Maternal blood vessel endothelial cells were positive, whereas maternal lacunae were lined with FSHR-negative trophoblasts surrounded by FSHR-positive decidual cells (Fig. 6B).

Potential Role of Fetoplacental FSHR in a Mouse Model

Like endothelial cells of the chorionic villi in the human term placenta, the vasculature of the labyrinth zone of mouse term placenta, the major site of maternal-fetal exchange, expresses FSHR protein (Fig. 7A). In an effort to determine potential functional ramifications of placental FSHR, we took advantage of a mouse model in which the *Fshr* is globally knocked out [19], performing the following experiments. We crossed $Fshr^{+/-}$ males to females, which would theoretically produce litters comprising $Fshr^{+/-}$ fetuses, $Fshr^{+/+}$ fetuses, and $Fshr^{-/-}$ fetuses. This is possible because, although $Fshr^{-/-}$ mice are infertile, $Fshr^{+/-}$ mice retain a reduced level of fertility [18]. Importantly, because most of the mouse placenta, including the labyrinth, is genetically dictated by the fetal genotype [21], when all pregnant dams are of the same genotype (in this case $Fshr^{+/-}$) it is possible to determine the extent to which deletion of *Fshr* from the fetal portion of the placenta affects fetal and placental development. These conditions therefore permit the analysis of fetoplacental growth as a function of the fetal *Fshr* genotype.

Fetoplacental units were collected from pregnant $Fshr^{+/-}$ females that had been mated with $Fshr^{+/-}$ males at midgestation (14–16 dpc). The fetus and placenta were then separated and weighed, and the fetus was genotyped. For each pregnant dam, the weights of the fetuses were normalized to the mean weight of the $Fshr^{+/-}$ fetuses in the same litter (unlike $Fshr^{+/+}$ fetuses, $Fshr^{+/-}$ were present in all litters), and those of the placentae were normalized to the mean weight of placentae from $Fshr^{+/-}$ fetuses in the same litter. Normalized data for fetuses and placentae from all pregnant dams (9 pregnancies and 54 fetoplacental units) were then pooled and analyzed. As expected, placentae associated with $Fshr^{-/-}$ mice did not express FSHR, as determined by immunostaining (Fig. 7B). The placentae associated with *Fshr* null and heterozygous fetuses each exhibited a 30% decrease in weight compared with placentae from their wild-type littermates (Fig. 8A). Thus,

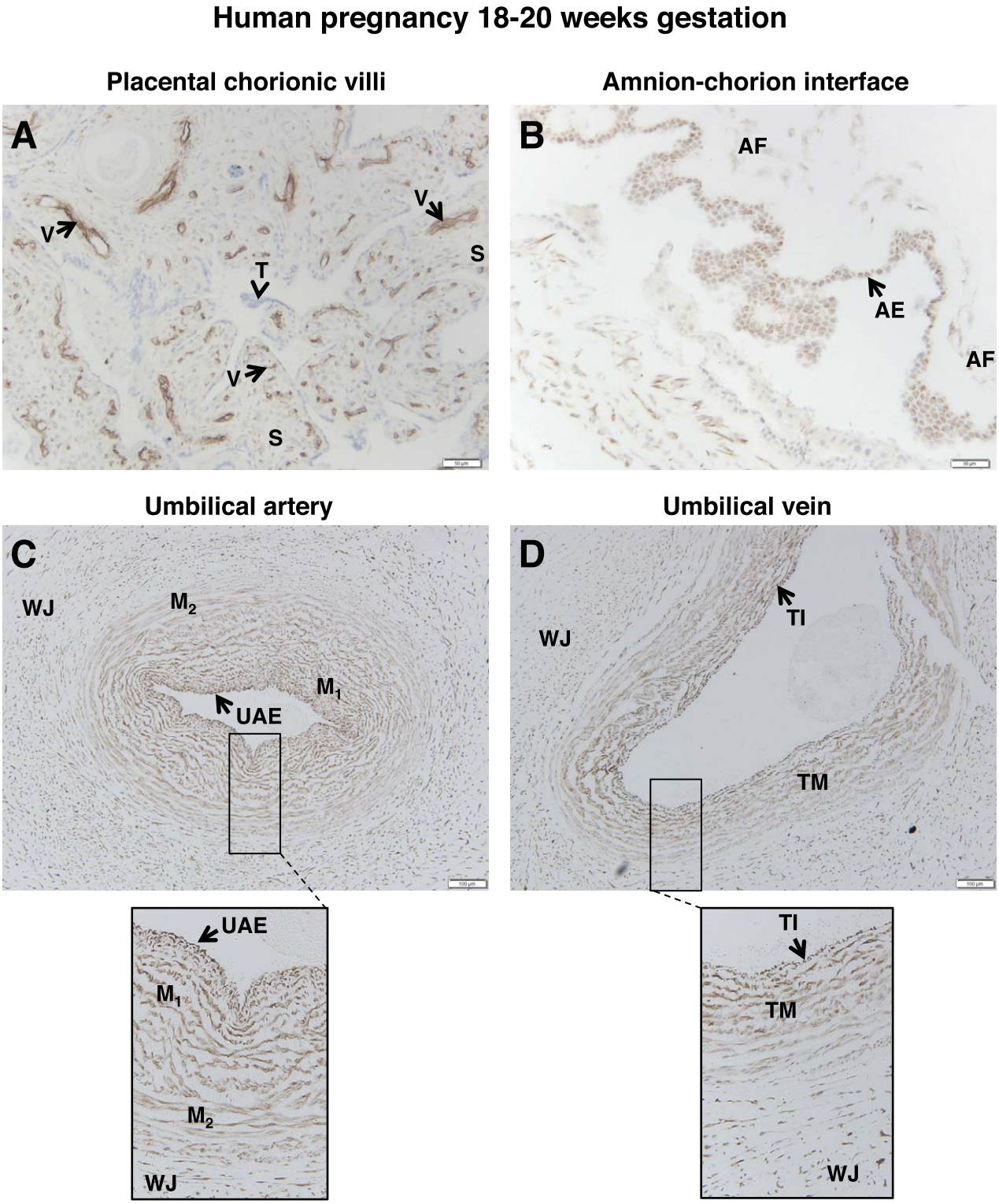

FIG. 4. FSHR expression in human placenta and associated tissues at 18–20 wk gestation. Tissues were stained with antibody FSHR-323 IgG2a (brown) and counterstained with hematoxylin (blue). **A**) Chorionic villi (magnification ×200). Labeled are endothelial cells of the developing villi vessels (V), the chorionic stromal core (S), and trophoblasts (arrowhead labeled T). **B**) Amnion-chorion interface (magnification ×200). Labeled are the amniotic epithelium (AE) and amniotic fibroblasts (AF). **C**) Umbilical artery (magnification ×100; inset ×200). Labeled are the umbilical artery epithelium (UAE), smooth muscle layers (M), and Wharton jelly (WJ). **D**) Umbilical vein (magnification ×100; inset ×200). Labeled are the endothelial tunica intima (TI), the tunica media (TM), and Wharton jelly (WJ). Corresponding negative controls stained with nonimmune IgG2a at the same concentration are shown in Supplemental Figure S5.

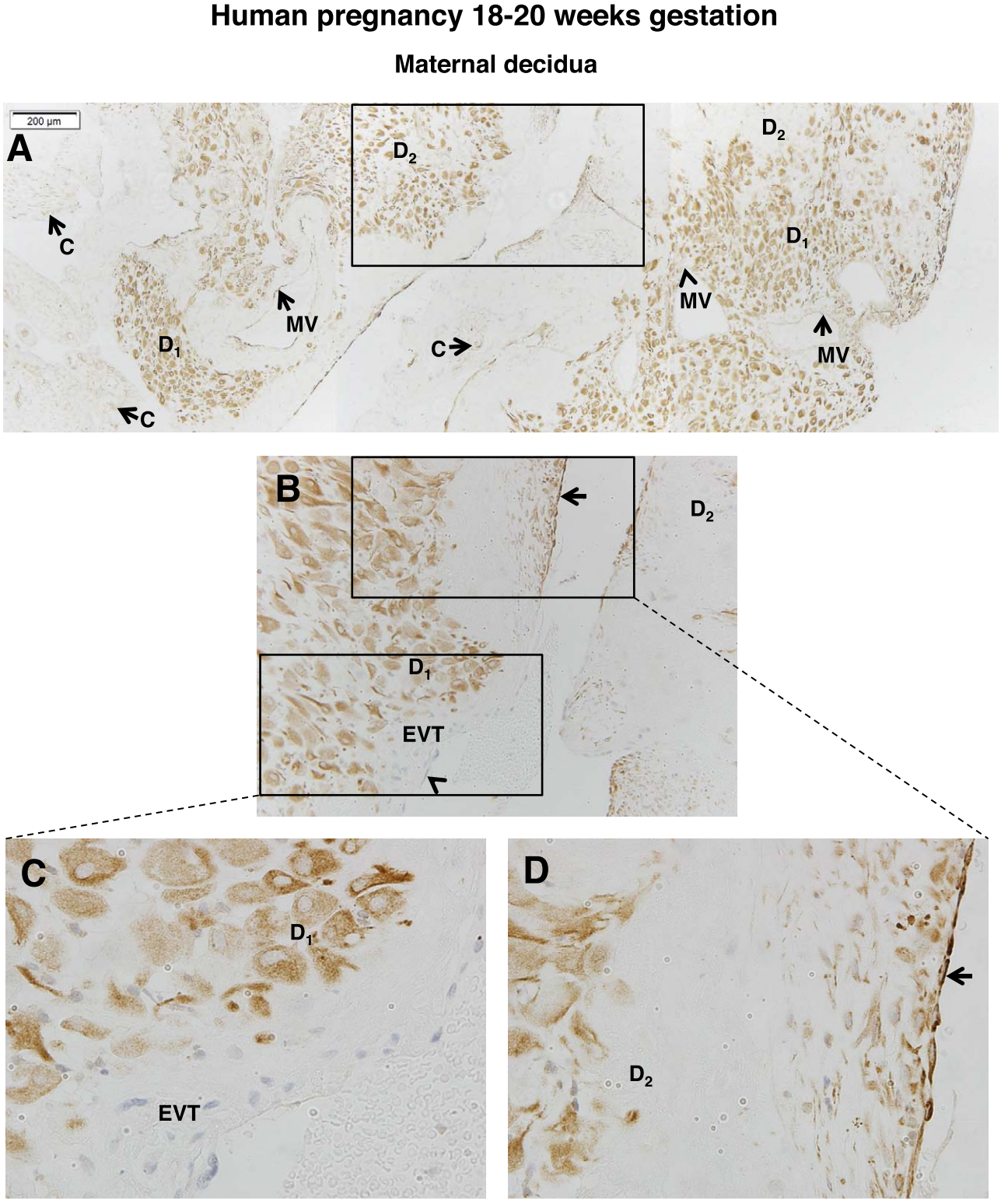

FIG. 5. FSHR expression in human decidua at 18–20 wk gestation. Tissues were stained with antibody FSHR-323 IgG2a (brown) and counterstained with hematoxylin (blue). Shown in **A**–**D** is the maternal decidua. **A**) A tiling of adjacent images taken at magnification ×100. **B**) Magnified image (magnification ×200) of the area enclosed by the rectangle in **A**. **C**) A magnified image (magnification ×600) of the area enclosed by the lower rectangle in **B**. **D**) A magnified image (magnification ×600) of the area enclosed by the upper rectangle in **B**. Labeled are decidual cells with relatively high FSHR expression (D_1), decidual cells with lower FSHR expression (D_2), chorionic villi (C), extravillous trophoblasts (EVT), and maternal vessels (MV). Arrows indicate maternal vessels that are positive for FSHR expression, and arrowheads indicate MVs that are negative for FSHR expression. Negative controls stained with nonimmune IgG2a at the same concentration are shown in Supplemental Figure S6.

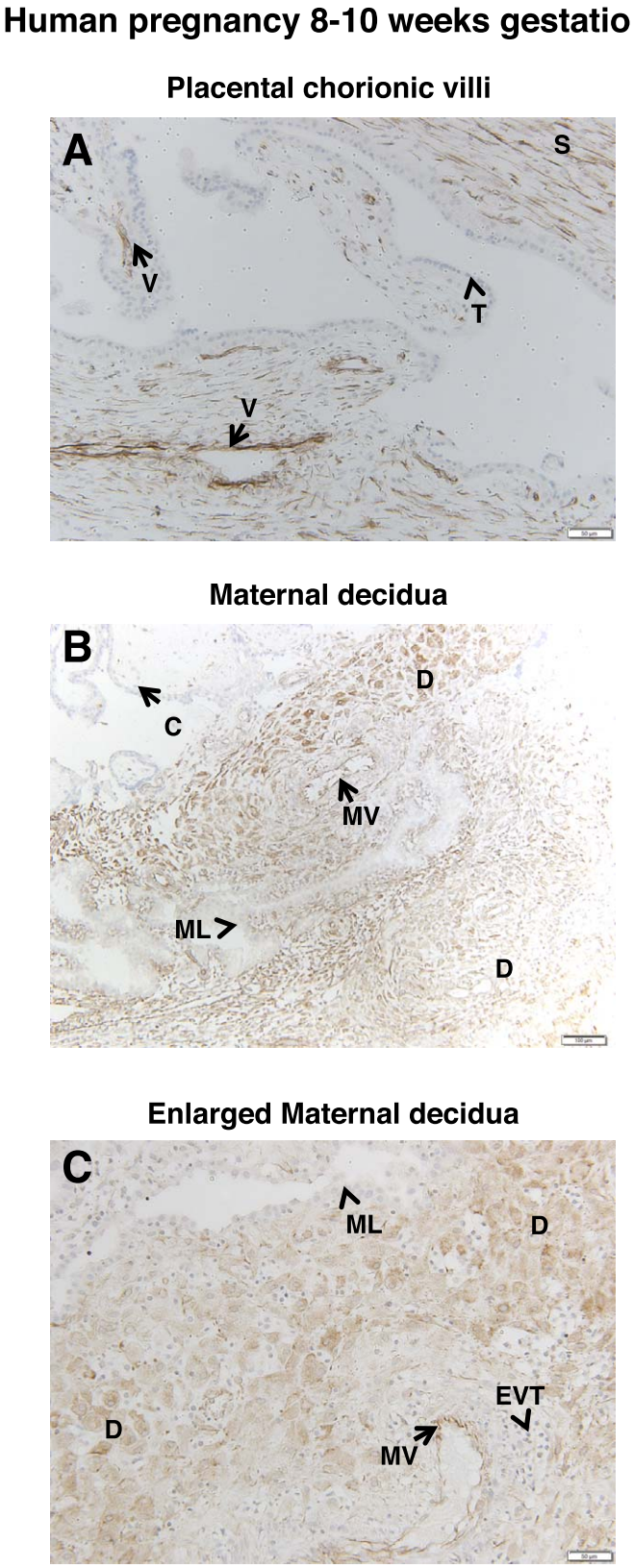

FIG. 6. FSHR expression in human placenta and associated tissues at 8–10 wk gestation. Tissues were stained with antibody FSHR-323 IgG2a (brown) and counterstained with hematoxylin (blue). **A**) Chorionic villi (magnification ×200). Labeled are endothelial cells of developing chorionic villi vessels (V), the chorionic stromal core (S), and trophoblasts (arrowheads labeled T). **B** and **C**) Maternal decidua (magnifications ×100 [**B**] and ×200 [**C**]). Labeled are decidua (D), maternal vessels (MV), maternal lacunae (ML), and chorionic villi (C). Extravillous trophoblasts are labeled EVT in **C**. Corresponding negative controls stained with nonimmune IgG2a at the same concentration are shown in Supplemental Figure S7.

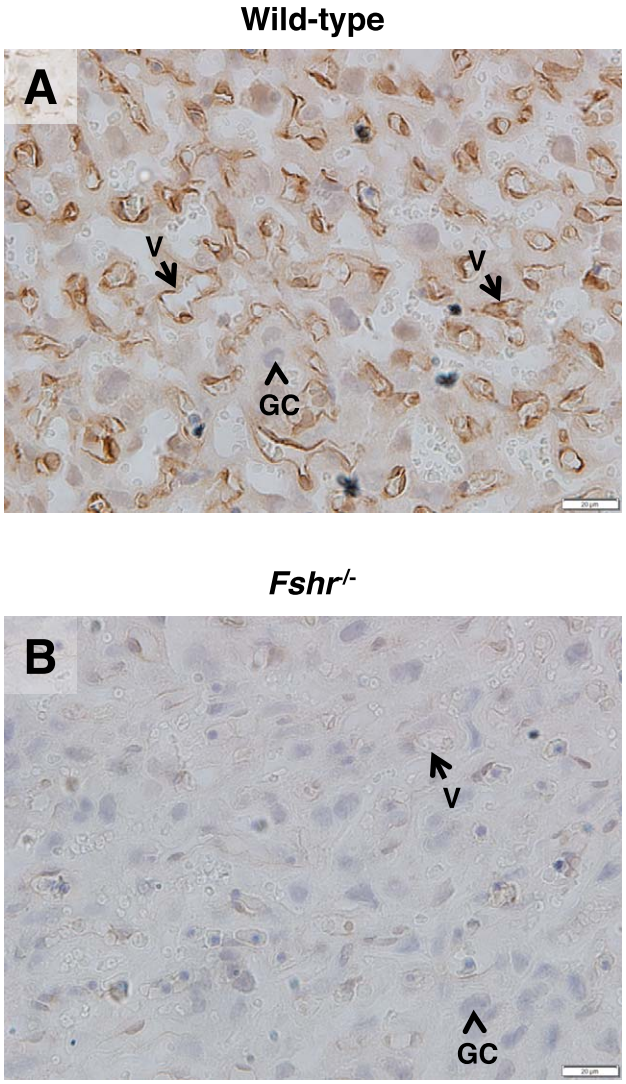

FIG. 7. FSHR expression in the labyrinth layer of mouse placenta. The labyrinth layer of placentae (15 dpc) of littermate wild-type (**A**) and *Fshr*$^{-/-}$ (**B**) mice were stained with anti-rat FSHR antibody. Images are shown at magnification ×600. Labeled are endothelial cells of mouse placental blood vessels (arrow labeled V) and mouse placental giant cells (arrowhead labeled GC). Corresponding negative controls stained with preimmune serum at the same concentration are shown in Supplemental Figure S8.

haploinsufficiency of fetoplacental *Fshr* significantly blunted placental growth, and ablation of both fetoplacental *Fshr* alleles caused no further attenuation of placental growth. The weights of *Fshr*$^{-/-}$ fetuses were also significantly (21%) lower than wild-type littermate fetuses (Fig. 8B), consistent with a restriction of fetal growth as a consequence of a lack of fetoplacental FSHR. Although the fetal weights of the heterozygotes exhibited a trend towards a reduction relative to those of their wild-type littermates (12%), this difference did

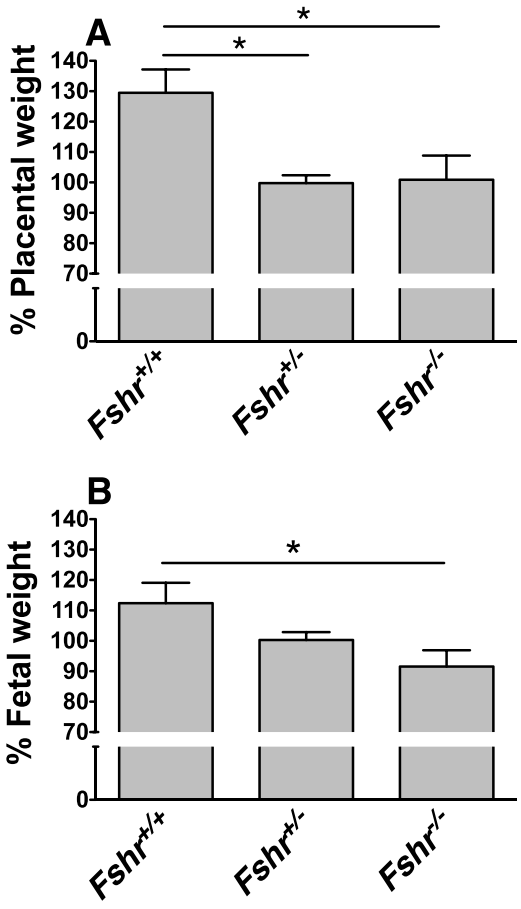

C

Fetal *Fshr* Genotype	% Fetuses (n=54)
Fshr$^{+/+}$	30.4
Fshr$^{+/-}$	50.0
Fshr$^{-/-}$	19.6

FIG. 8. *Fshr* genotype-specific differences in fetoplacental development among littermates. *Fshr*$^{+/-}$ females were mated with *Fshr*$^{-/-}$ males, and at 14–16 dpc, fetoplacental units were dissected and analyzed as described in *Materials and Methods*. **A**) Quantification of placental weight as a function of fetal *Fshr* genotype. Data are expressed as a percentage of the mean weight of littermate *Fshr*$^{+/-}$ placentae. **B**) Quantification of fetal weight as a function of fetal *Fshr* genotype. Data are expressed as a percentage of the mean weight of littermate *Fshr*$^{+/-}$ fetuses. Data shown in **A** and **B** are the mean ± SEM for 54 pups from 9 litters. Asterisks denote a difference of $P < 0.05$. **C**) Percentage of fetuses of each *Fshr* genotype.

not reach statistical significance. Finally, at midgestation there were fewer *Fshr*$^{-/-}$ fetuses and more wild-type fetuses than would be expected according to Mendelian inheritance (Fig. 8C). Furthermore, in three of the litters in which fetal loss was detectable (at 14 dpc), the tissue that remained was adequate for genotyping; all of these fetuses were of the *Fshr*$^{+/-}$ phenotype. Taken together, these results indicate that normal placental and fetal development requires fetoplacental *Fshr*.

Localization of FSHR in Human Nonpregnant Reproductive Tissues

Because FSHR expression was observed in the decidual layer of the pregnant uterus in women, we sought to determine whether it is also expressed in the uterus of nonpregnant women. Nonpregnant endometrium was examined in both the proliferative and secretory phases. In the proliferative phase, endometrial glands throughout the glandular epithelium stained intensely for FSHR (Fig. 9A). In addition, endometrial blood vessels exhibited a strong FSHR signal, and the endometrial stroma exhibited a moderate one. In the secretory-phase endometrium, the glands were also positive for FSHR but, notably, often only at the base of the glandular epithelium (Fig. 9B). Furthermore, FSHR expression in the stroma seemed to be lower in this context, whereas that in the endometrial blood vessels remained strong.

Nonpregnant cervix was also examined. FSHR staining was intense in both the glandular epithelium and the cervical muscle fibers (Fig. 9C). With regard to the blood vessels, FSHR was also present in both the endothelial cells and arterial smooth muscle (Fig. 7D).

Localization of FSHR in Human Nonpregnant Versus Pregnant Myometrium

Nonpregnant myometrium was also examined for expression patterns of FSHR (Fig. 10A). These findings were consistent with those for the nonpregnant cervix in that both the endothelial cells in the myometrial vessels and arterial smooth muscle were positive. However, in this case only a weak signal was detected in the muscle fibers.

To determine whether FSHR in the myometrial muscle fibers remains low during pregnancy, we examined myometrium samples from women at term. As shown in Figure 10B, FSHR staining was strong not only in the endothelial cells and arterial smooth muscle, but also in the muscle fibers. The results shown in Figure 10, A and B, are representative of samples from three nonpregnant and three pregnant (term) women, respectively, and were processed together. The immunohistochemical data from all six samples were quantified for relative levels of FSHR specifically in the muscle fibers and stroma (i.e., excluding signal in the endothelial cells of the blood vessels). This analysis revealed that FSHR levels in the muscle fibers and stroma of pregnant (term) myometrium were nearly 10-fold higher than those in nonpregnant myometrium (Fig. 10C).

Human myometrium from term pregnancy was further examined for the presence of FSHR mRNA. Polymerase chain reaction amplification of exons 2–3 of *FSHR* mRNA, a region common to the full-length *FSHR* mRNA (the form most prevalent in ovary) and most known *FSHR* mRNA splice variants [8–10, 15], revealed a band of the expected size (Fig. 11A). Splice variants lacking exon 2 (Fig. 11B), exon 6 (Fig. 11C), or exon 9 (Fig. 11D) were not detected. Therefore, in contrast to endothelial cells, which express *FSHR* mRNA as a splice variant lacking exon 9 [8], myometrium expresses full-length *FSHR* mRNA.

Messenger RNAs Encoding FSH Subunits in Human Extragonadal Reproductive Tissues

Although it is feasible to view pituitary FSH exerting actions on FSHR in the extragonadal reproductive tissues of nonpregnant women, it is difficult to envision similar endocrine actions of FSH on the extragonadal reproductive tissues of

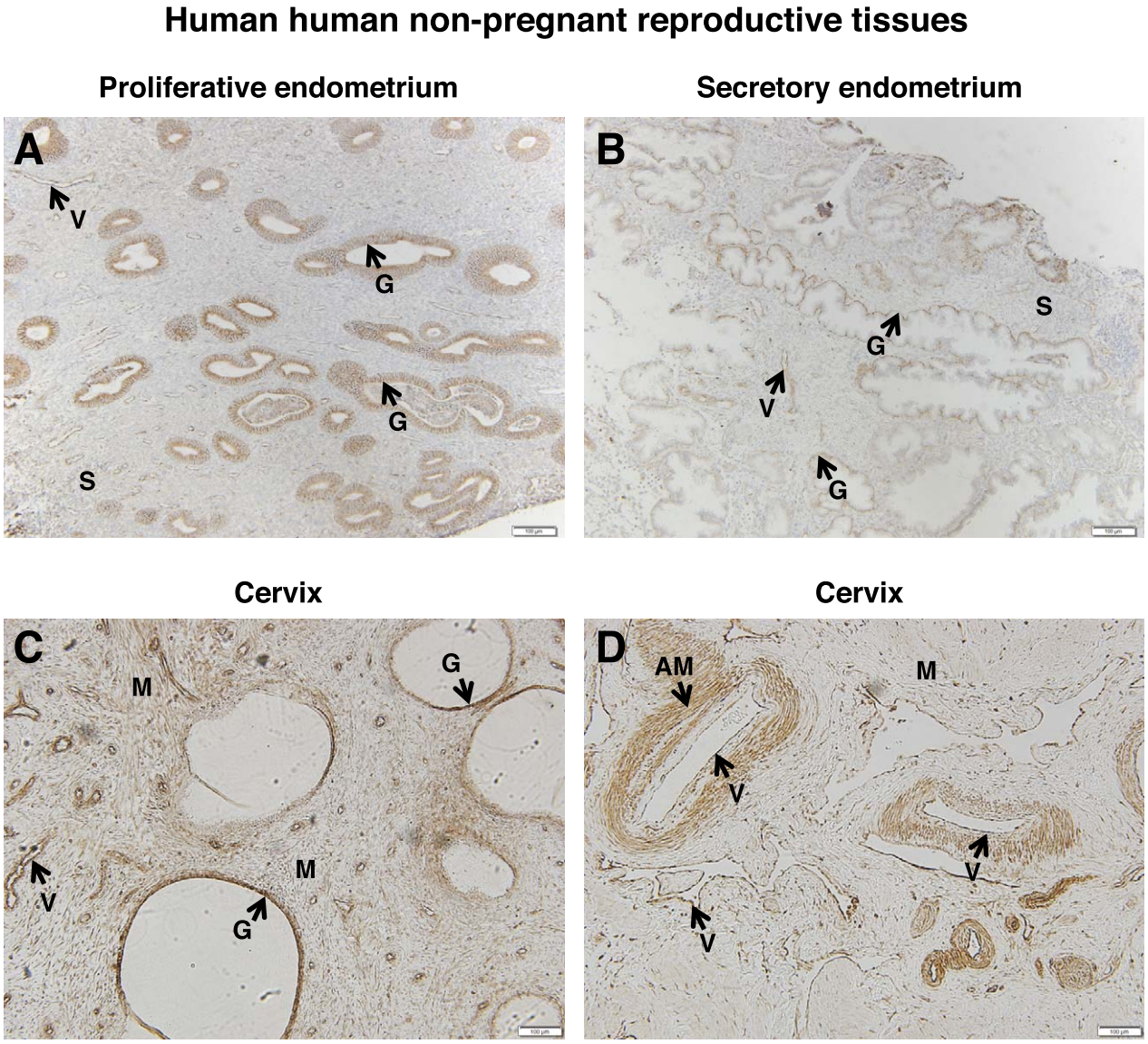

FIG. 9. FSHR expression in human nonpregnant reproductive tissues. Tissues were stained with antibody FSHR-323 IgG2a (brown) and counterstained with hematoxylin (blue). **A**) Proliferative endometrium (magnification ×100). Labeled are glandular epithelium (G), endometrial stroma (S), and endothelial cells of an endometrial blood vessel (V). **B**) Secretory endometrium (magnification ×100). Labeled are glandular epithelium (G), endometrial stroma (S), and endothelial cells of the endometrial blood vessels (V). **C** and **D**) Cervix (magnification ×100). Labeled are cervical glands (G), cervical muscle (M), endothelial cells of cervical blood vessels (V), and arterial smooth muscle (AM). Corresponding negative controls stained with nonimmune IgG2a at the same concentration are shown in Supplemental Figure S9.

pregnant women because maternal FSH is suppressed during pregnancy [22]. Therefore, in light of reported paracrine effects of oxytocin on the pregnant uterus [23, 24], we sought to determine whether during pregnancy FSH might be synthesized locally, where it could act by paracrine or autocrine mechanisms on the placenta and uterus. To this end, we examined uteroplacental tissue (including the maternal decidua and placenta), placenta (maternal decidua and amnion removed), maternal uterine decidua, and uterine myometrium from term pregnancy, as well as HUVECs, for the potential presence of mRNAs encoding the β subunit of FSH (from the *FSHB* gene) and the common glycoprotein α subunit (from the *CGA* gene), including human pituitary as a positive control. As shown in Figure 12, uteroplacental tissue, placenta, decidua, and myometrium, but not HUVECs, revealed expression of the *FSHB* and *CGA* genes, providing evidence for the potential local synthesis of FSH in these tissues.

DISCUSSION

Our results demonstrate that FSHR protein is expressed not only in ovarian granulosa cells, as is well documented, but also in numerous other cell types of the female reproductive tract. Furthermore, they reveal that during pregnancy FSHR is expressed in the placenta, umbilical cord, amnion, and maternal decidua.

With respect to the human placenta, FSHR was present in the endothelial cells of chorionic villi at term, as well as in those of the developing villi by 8–10 wk gestation (the earliest time point examined), suggesting that endothelial FSHR may contribute to development of the placental vasculature. Consistent with this premise, we previously showed that primary cultures of HUVECs express FSHR and respond to FSH with the stimulation of several angiogenic processes, including the formation of tubelike structures, with an efficacy similar to that of VEGF [8]. Proper development of the

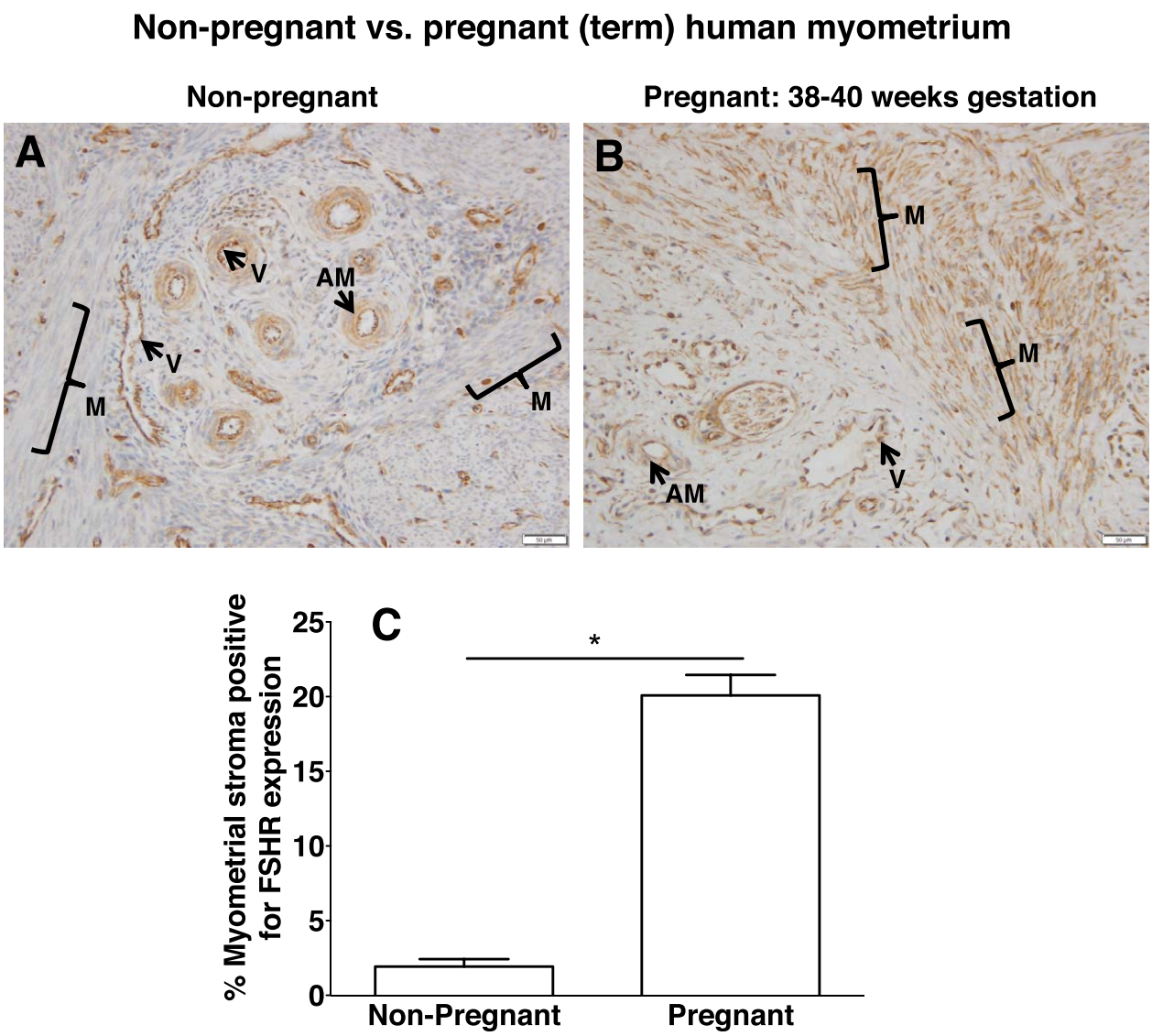

FIG. 10. Differential expression of FSHR in human myometrial stroma of nonpregnant versus pregnant (term) uterus. Tissues in **A** (nonpregnant myometrium) and **B** (pregnant myometrium at 38–40 wk gestation) were stained with antibody FSHR-323 IgG2a (brown) and counterstained with hematoxylin (blue) and are shown at magnification ×200. Labeled are myometrial muscle fibers (M with bracket), myometrial blood vessels (V), and arterial smooth muscle (AM). Images in **A** and **B** are representative of samples from three nonpregnant women and three pregnant (term) women, respectively. Corresponding negative controls stained with nonimmune IgG2a at the same concentration are shown in Supplemental Figure S10. **C**) Quantitation of FSHR expression in muscle (excluding that in blood vessels) from all of the nonpregnant and pregnant (term) samples, based on immunohistochemical staining of all slides in the same experiment and quantification as described in *Materials and Methods*. Data shown are the mean ± SEM. Asterisk denotes a difference of $P < 0.05$.

placental vasculature during pregnancy is essential for sufficient transplacental exchange, and thus for the support of normal fetal growth. Indeed, insufficient placental vascularization has been associated with early embryonic mortality and with intrauterine growth retardation and/or preeclampsia [25–32].

The results of our experiments presented herein using genetically altered mice are consistent with the premise that the presence of FSHR in the placenta is essential for normal pregnancy. All of the pregnant females used in analyzing fetoplacental growth as a function of fetal *Fshr* genotype (which dictates the genetic composition of most of the mouse placenta, including the labyrinth) were haploinsufficient, ensuring any adverse pregnancy outcomes pertaining specifically to parental genotype would not affect the conclusions from this particular comparative study. The decrease in fetal and placental weights observed at midgestation (14–16 dpc) in the case of the fetoplacental $Fshr^{-/-}$ genotype suggests that the absence of FSHR leads to growth restriction. Interestingly, even haploinsufficiency of placental *Fshr* resulted in decreased placental weight and a trend toward decreased fetal weight. These observations suggest that, unlike the ovary, the placenta expressed FSHR at relatively low levels and therefore does not express spare FSHR. This presumption is consistent with our findings in HUVECs, where we detected relatively low densities of FSHR by ^{125}I-FSH-binding assays and relatively low levels of *FSHR* mRNA [8].

Moreover, our observation of a low percentage of $Fshr^{-/-}$ fetuses accompanied by a high percentage of $Fshr^{+/+}$ fetuses with respect to Mendelian ratios indicates that this condition contributes to the demise of the fetuses and affects the $Fshr^{+/-}$ fetuses to some extent. Although previous studies in which

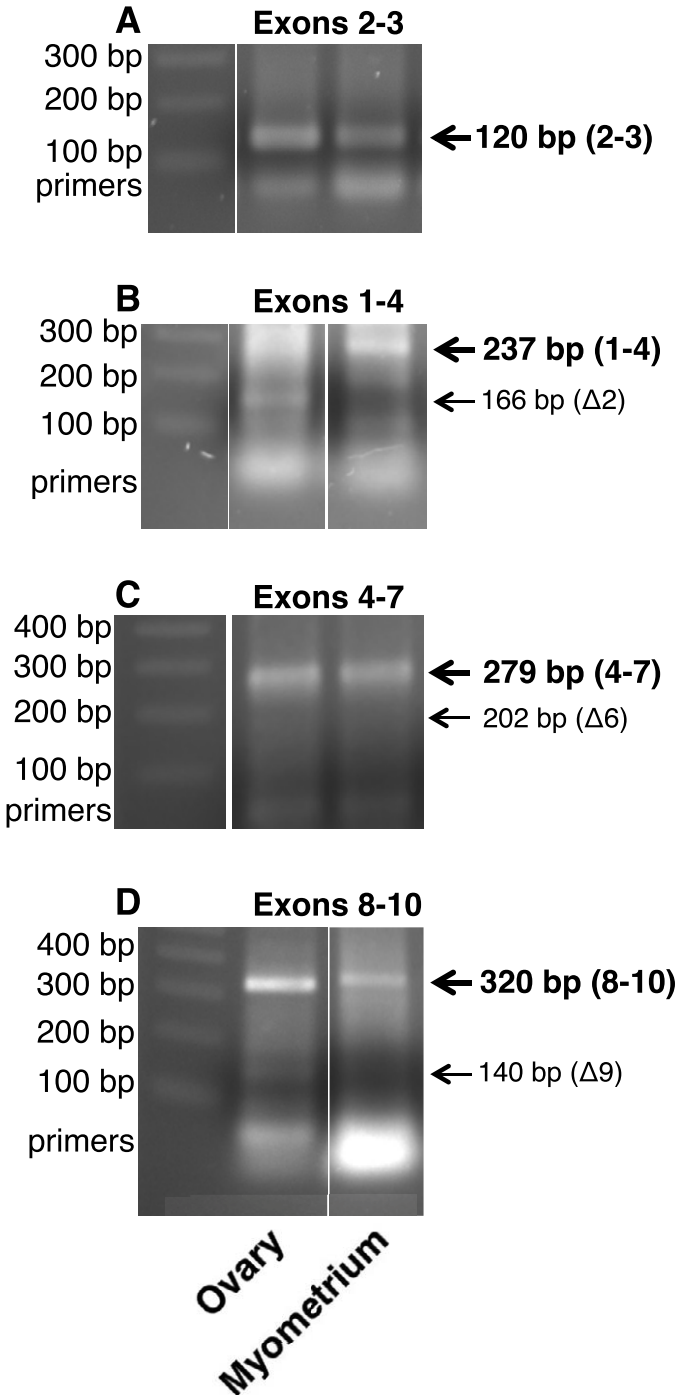

FIG. 11. *FSHR* mRNA in human term myometrium. RNAs from human myometrium from one patient at term pregnancy and from pooled human ovaries were examined for *FSHR* mRNA transcripts as described in *Materials and Methods*. *FSHR* mRNA from exons 2–3 (**A**), exons 1–4 (**B**), exons 4–7 (**C**), and exons 8–10 (**D**) indicated the presence of full-length FSHR mRNA and the absence of *FSHR* mRNA splice variants lacking exons 2, 6, or 9, respectively, in myometrium. Each panel represents data from one gel. In a given panel, spaces between images represent where one or more lanes containing irrelevant data were excised from the figure.

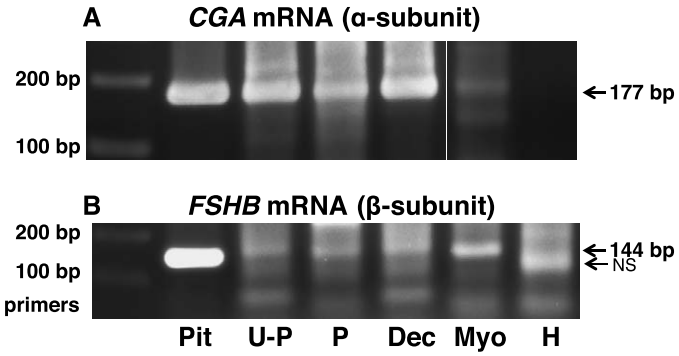

FIG. 12. Messenger RNAs encoding FSH subunits are present in extragonadal reproductive tissues. Polymerase chain reaction was used to amplify *CGA* mRNA encoding the glycoprotein α subunit (**A**) and FSHB mRNA encoding the β subunit of FSH (**B**) in human tissues, as described in *Materials and Methods*. Human tissues from term pregnancy included uteroplacental tissue (U-P), placenta (P; maternal decidua and amnion removed), uterine decidua (Dec), and uterine myometrium (Myo). The HUVECs (H) were also analyzed. Human pituitary (Pit) was included as a positive control. Each panel represents data from one gel. In a given panel, spaces between images represent where one or more lanes containing irrelevant data were excised from the figure.

$Fshr^{+/-}$ mice were intercrossed stated that the pattern of inheritance was Mendelian [17, 33], in the instance where the data were presented the numbers were consistent with our observations of a high ratio of $Fshr^{+/+}$ fetuses at the expense of their $Fshr^{-/-}$ counterparts [33]. Notably, the fetal remnants identified at 14 dpc in our study were all of the $Fshr^{+/-}$ genotype, leading us to speculate that reabsorption of the $Fshr^{-/-}$ fetuses occurs earlier in gestation. Collectively, the data presented herein and in our report on HUVECs [8] suggest that endothelial cell FSHR in the placental vasculature promotes angiogenesis, and that insufficient signaling through the placental endothelial FSHR has an adverse effect on growth of both the fetus and the placenta.

Our analysis also revealed that during pregnancy, FSHR is expressed in several other tissues: the umbilical cord (endothelial cells of the blood vessels and smooth muscle surrounding the artery), the amnion (epithelial cells and the stroma), and the maternal decidua (decidual cells and endothelial cells of the blood vessels). The presence of FSHR in the endothelial cells of umbilical cord blood vessels suggests a potential role in mediating the significant increase in maternal-fetal blood flow that is required for a successful pregnancy [31, 34]. In the case of the placenta-associated maternal decidua, the pattern of FSHR expression was particularly intriguing. Specifically, the observation of high levels of FSHR in clusters of decidual cells was distinct from the pattern in nonpregnant endometrium, where FSHR was highly expressed in the glands but at relatively low levels in the stroma.

With respect to FSHR in the decidua, we note that a microarray study by Popovici et al. [5] revealed that FSHR mRNA increased in human endometrial stromal cells decidualized with progesterone or cAMP. Furthermore, adding FSH to stromal cells isolated from proliferative human endometrium has been reported to induce a decidual phenotype that includes expression of the prolactin receptor [35]. Our findings documenting FSHR protein expression in human decidual cells extend these earlier studies and highlight the nonhomogeneous nature of FSHR expression in the decidua. The observed expression of FSHR in the endothelial cells of maternal blood vessels in the decidua is likewise notable. In particular, it is striking that at 18–20 wk gestation the maternal spiral arteries, which appeared to be undergoing remodeling based on the presence of extravillous trophoblasts, were themselves negative for FSHR but were surrounded by decidual cells that were intensely positive. Based on this

observation, we speculate that cross talk between the decidual cells and spiral arteries coordinates FSHR expression to promote an environment optimal for vessel remodeling. Collectively, the expression patterns of FSHR in the maternal decidua suggest that this receptor may play heretofore unappreciated roles in implantation of the embryo and in remodeling the maternal spiral arteries.

The data presented here also reveal FSHR in the glands and smooth muscle of nonpregnant human cervix as well. The roles of cervical FSHR in nonpregnancy and pregnancy remain to be elucidated. In contrast to cervical smooth muscle in nonpregnant women, myometrial smooth muscle in this population was found to express very little FSHR protein. However, in pregnant myometrium at term, the levels of FSHR were ~10-fold higher. Previous studies showed that applying FSH to the myometrium of nonpregnant adult rats suppresses spectral components of myoelectrical signals, consistent with FSH playing a role in the suppression of uterine activity in the nonpregnant state [6, 7]. Important outstanding questions are whether the effects of FSH on the myometrium differ in the nonpregnant and pregnant states, and among different gestational stages during pregnancy.

Notably, a recent study identified *FSHR* as a gene involved in the timing of birth in humans, and showed that intronic single-nucleotide polymorphisms in this gene are associated with preterm birth [11]. The expression patterns of FSHR protein reported in the current study identify the cervix, myometrium, and amnion as extragonadal sites that could potentially contribute to the timing of parturition.

Although FSHR protein is detected by immunostaining in various tissues of the female reproductive tract, the immunostaining does not inform us regarding whether it is the full-length FSHR and/or a splice variant of the receptor that is expressed [8–10, 15]. As shown herein, human myometrium from term pregnancy expresses the full-length *FSHR* mRNA, the form most abundant in ovary. In contrast, HUVECs do not express the full-length *FSHR* mRNA, but rather a splice variant lacking exon 9 [8]. FSHR(Δ9) is functional, as demonstrated by the FSH stimulation of angiogenic processes in HUVECs [8] and by FSH-stimulated bone loss mediated by osteoclasts, both of which similarly express only FSHR(Δ9) [1, 2]. It remains to be determined which form(s) of FSHR are expressed in other cells of the female reproductive tract.

The premise that extragonadal FSHR is important for a healthy pregnancy demands that there be locally produced FSH, because maternal pituitary FSH secretion is inhibited during pregnancy [22]. In such a scenario, relatively low concentrations of FSH that may have gone largely undetected to date could be sufficient to exert physiologically relevant paracrine effects. A precedent for regulation of this type comes from the study of oxytocin, a known regulator of parturition that is frequently used to stimulate labor clinically; this hormone is thought to exert its effects through paracrine, rather than endocrine, mechanisms [23, 24]. Indeed, oxytocin is synthesized in the decidua and, to a lesser extent, the chorion and amnion [24, 36, 37]. We postulate that FSH may function similarly, being produced at low concentrations in the uterus and/or placenta, where it can exert local effects. Data presented reveal that both *FSHB* mRNA (encoding FSHβ) and *CGA* mRNA (encoding the common α subunit) are present in the placental chorionic plate and uterine decidua from term placenta (amnion was not examined) as well as pregnant term myometrium. Neither subunit was detected in HUVECs, suggesting that FSHR in the endothelial cells of the placental vasculature is likely responding via paracrine mechanisms to FSH produced in other cells within the placenta. Interestingly, decidua and myometrium each express FSHR as well as *FSHB* and *CGA* mRNAs, suggesting paracrine and/or autocrine actions of FSH in those tissues. Additional data supporting the expression of *FSHB* and *CGA* genes in uteroplacental tissues are within microarray data deposited with the National Center for Biotechnology Information's GEO [38–47].

In conclusion, it should be noted that a population-based cohort study of women revealed that increased risks for small for gestational age babies, premature births, and perinatal deaths were attributable to factors leading to infertility or subfertility and not to factors related to assisted reproductive technology [48]. Decreased signaling through the FSHR can, of course, contribute to infertility or subfertility by virtue of the role of ovarian FSHR in promoting follicular growth. Therefore, in light of our studies, it is provocative to consider that if a women with attenuated FSHR signaling were to achieve pregnancy, decreased FSHR signaling in extragonadal tissues may increase her risk for adverse pregnancy outcomes.

ACKNOWLEDGMENT

The authors thank Christine Blaumueller for critical review of the manuscript.

REFERENCES

1. Sun L, Peng Y, Sharrow AC, Iqbal J, Zhang Z, Papachristou DJ, Zaidi S, Zhu LL, Yaroslavskiy BB, Zhou H, Zallone A, Sairam MR, et al. FSH directly regulates bone mass. Cell 2006; 125:247–260.
2. Zhu LL, Blair H, Cao J, Yuen T, Latif R, Guo L, Tourkova IL, Li J, Davies TF, Sun L, Bian Z, Rosen C, et al. Blocking antibody to the beta-subunit of FSH prevents bone loss by inhibiting bone resorption and stimulating bone synthesis. Proc Natl Acad Sci U S A 2012; 109: 14574–14579.
3. Radu A, Pichon C, Camparo P, Antoine M, Allory Y, Couvelard A, Fromont G, Hai MT, Ghinea N. Expression of follicle-stimulating hormone receptor in tumor blood vessels. N Engl J Med 2010; 363: 1621–1630.
4. Mizrachi D, Shemesh M. Follicle-stimulating hormone receptor and its messenger ribonucleic acid are present in the bovine cervix and can regulate cervical prostanoid synthesis. Biol Reprod 1999; 61:776–784.
5. Popovici RM, Kao LC, Giudice LC. Discovery of new inducible genes in in vitro decidualized human endometrial stromal cells using microarray technology. Endocrinology 2000; 141:3510–3513.
6. Celik O, Tagluk ME, Hascalik S, Elter K, Celik N, Aydin NE. Spectrotemporal changes in electrical activity of myometrium due to recombinant follicle-stimulating hormone preparations follitropin alfa and beta. Fertil Steril 2008; 90:1348–1356.
7. Hascalik S, Celik O, Tagluk ME, Yildirim A, Aydin NE. Effects of highly purified urinary FSH and human menopausal FSH on uterine myoelectrical dynamics. Mol Hum Reprod 2010; 16:200–206.
8. Stilley JA, Guan R, Duffy DM, Segaloff DL. Signaling through FSH receptors on human umbilical vein endothelial cells promotes angiogenesis. J Clin Endocrinol Metab 2014; 99:E813–E820.
9. Robinson LJ, Tourkova I, Wang Y, Sharrow AC, Landau MS, Yaroslavskiy BB, Sun L, Zaidi M, Blair HC. FSH-receptor isoforms and FSH-dependent gene transcription in human monocytes and osteoclasts. Biochem Biophys Res Commun 2010; 394:12–17.
10. Zhu LL, Tourkova I, Yuen T, Robinson LJ, Bian Z, Zaidi M, Blair HC. Blocking FSH action attenuates osteoclastogenesis. Biochem Biophys Res Commun 2012; 422:54–58.
11. Plunkett J, Doniger S, Orabona G, Morgan T, Haataja R, Hallman M, Puttonen H, Menon R, Kuczynski E, Norwitz E, Snegovskikh V, Palotie A, et al. An evolutionary genomic approach to identify genes involved in human birth timing. PLoS Genet 2011; 7:e1001365.
12. Vannier B, Loosfelt H, Meduri G, Pichon C, Milgrom E. Anti-human FSH receptor monoclonal antibodies: immunochemical and immunocytochemical characterization of the receptor. Biochemistry 1996; 35: 1358–1366.
13. Quintana J, Hipkin RW, Ascoli M. A polyclonal antibody to a synthetic peptide derived from the rat follicle-stimulating hormone receptor reveals

the recombinant receptor as a 74-kilodalton protein. Endocrinology 1993; 133:2098–2104.
14. Zhang M, Guan R, Segaloff DL. Revisiting and questioning functional rescue between dimerized LH receptor mutants. Mol Endocrinol 2012; 26: 655–668.
15. Gerasimova T, Thanasoula MN, Zattas D, Seli E, Sakkas D, Lalioti MD. Identification and in vitro characterization of follicle stimulating hormone (FSH) receptor variants associated with abnormal ovarian response to FSH. J Clin Endocrinol Metab 2010; 95:529–536.
16. Bieche I, Latil A, Parfait B, Vidaud D, Laurendeau I, Lidereau R, Cussenot O, Vidaud M. CGA gene (coding for the alpha subunit of glycoprotein hormones) overexpression in ER alpha-positive prostate tumors. Eur Urol 2002; 41:335–341.
17. Danilovich N, Babu PS, Xing W, Gerdes M, Krishnamurthy H, Sairam MR. Estrogen deficiency, obesity, and skeletal abnormalities in follicle-stimulating hormone receptor knockout (FORKO) female mice. Endocrinology 2000; 141:4295–4308.
18. Danilovich N, Sairam MR. Haploinsufficiency of the follicle-stimulating hormone receptor accelerates oocyte loss inducing early reproductive senescence and biological aging in mice. Biol Reprod 2002; 67:361–369.
19. Dierich A, Sairam MR, Monaco L, Fimia GM, Gansmuller A, LeMeur M, Sassone-Corsi P. Impairing follicle-stimulating hormone (FSH) signaling in vivo: targeted disruption of the FSH receptor leads to aberrant gametogenesis and hormonal imbalance. Proc Natl Acad Sci U S A 1998; 95:13612–13617.
20. Whitten WK. Modification of the oestrous cycle of the mouse by external stimuli associated with the male. J Endocrinol 1956; 13:399–404.
21. Rossant J, Croy BA. Genetic identification of tissue of origin of cellular populations within the mouse placenta. J Embryol Exp Morphol 1985; 86: 177–189.
22. Jaffe RB, Lee PA, Midgley AR Jr. Serum gonadotropins before, at the inception of, and following human pregnancy. J Clin Endocrinol Metab 1969; 29:1281–1283.
23. Terzidou V, Blanks AM, Kim SH, Thornton S, Bennett PR. Labor and inflammation increase the expression of oxytocin receptor in human amnion. Biol Reprod 2011; 84:546–552.
24. Mitchell BF, Fang X, Wong S. Oxytocin: a paracrine hormone in the regulation of parturition? Rev Reprod 1998; 3:113–122.
25. Ahmed A, Perkins J. Angiogenesis and intrauterine growth restriction. Baillieres Best Pract Res Clin Obstet Gynaecol 2000; 14:981–998.
26. Arroyo JA, Winn VD. Vasculogenesis and angiogenesis in the IUGR placenta. Semin Perinatol 2008; 32:172–177.
27. Garite TJ, Clark R, Thorp JA. Intrauterine growth restriction increases morbidity and mortality among premature neonates. Am J Obstet Gynecol 2004; 191:481–487.
28. Kinzler WL, Vintzileos AM. Fetal growth restriction: a modern approach. Curr Opin Obstet Gynecol 2008; 20:125–131.
29. Mayhew TM, Charnock-Jones DS, Kaufmann P. Aspects of human fetoplacental vasculogenesis and angiogenesis. III. Changes in complicated pregnancies.Placenta 2004; 25:127–139.
30. Barut F, Barut A, Gun BD, Kandemir NO, Harma MI, Harma M, Aktunc E, Ozdamar SO. Intrauterine growth restriction and placental angiogenesis. Diagn Pathol 2010; 5:24.
31. Khankin EV, Royle C, Karumanchi SA. Placental vasculature in health and disease. Semin Thromb Hemost 2010; 36:309–320.
32. Furuya M, Kurasawa K, Nagahama K, Kawachi K, Nozawa A, Takahashi T, Aoki I. Disrupted balance of angiogenic and antiangiogenic signalings in preeclampsia. J Pregnancy 2011; 2011:123717.
33. Abel MH, Wootton AN, Wilkins V, Huhtaniemi I, Knight PG, Charlton HM. The effect of a null mutation in the follicle-stimulating hormone receptor gene on mouse reproduction. Endocrinology 2000; 141: 1795–1803.
34. Reynolds LP, Borowicz PP, Caton JS, Vonnahme KA, Luther JS, Buchanan DS, Hafez SA, Grazul-Bilska AT, Redmer DA. Uteroplacental vascular development and placental function: an update. Int J Dev Biol 2010; 54:355–366.
35. Tang B, Gurpide E. Direct effect of gonadotropins on decidualization of human endometrial stroma cells. J Steroid Biochem Mol Biol 1993; 47: 115–121.
36. Mitchell BF, Wong S. Metabolism of oxytocin in human decidua, chorion, and placenta. J Clin Endocrinol Metab 1995; 80:2729–2733.
37. Chibbar R, Miller FD, Mitchell BF. Synthesis of oxytocin in amnion, chorion, and decidua may influence the timing of human parturition. J Clin Invest 1993; 91:185–192.
38. Huuskonen P, Storvik M, Reinisalo M, Honkakoski P, Rysa J, Hakkola J, Pasanen M. Microarray analysis of the global alterations in the gene expression in the placentas from cigarette-smoking mothers. Clin Pharmacol Ther 2008; 83:542–550.
39. Mikheev AM, Nabekura T, Kaddoumi A, Bammler TK, Govindarajan R, Hebert MF, Unadkat JD. Profiling gene expression in human placentae of different gestational ages: an OPRU Network and UW SCOR Study. Reprod Sci 2008; 15:866–877.
40. Votavova H, Dostalova Merkerova M, Fejglova K, Vasikova A, Krejcik Z, Pastorkova A, Tabashidze N, Topinka J, Veleminsky M, Jr., Sram RJ, Brdicka R. Transcriptome alterations in maternal and fetal cells induced by tobacco smoke. Placenta 2011; 32:763–770.
41. Winn VD, Haimov-Kochman R, Paquet AC, Yang YJ, Madhusudhan MS, Gormley M, Feng KT, Bernlohr DA, McDonagh S, Pereira L, Sali A, Fisher SJ. Gene expression profiling of the human maternal-fetal interface reveals dramatic changes between midgestation and term. Endocrinology 2007; 148:1059–1079.
42. Dezso Z, Nikolsky Y, Sviridov E, Shi W, Serebriyskaya T, Dosymbekov D, Bugrim A, Rakhmatulin E, Brennan RJ, Guryanov A, Li K, Blake J, et al. A comprehensive functional analysis of tissue specificity of human gene expression. BMC Biol 2008; 6:49.
43. Eyster KM, Klinkova O, Kennedy V, Hansen KA. Whole genome deoxyribonucleic acid microarray analysis of gene expression in ectopic versus eutopic endometrium. Fertil Steril 2007; 88:1505–1533.
44. Hawkins SM, Creighton CJ, Han DY, Zariff A, Anderson ML, Gunaratne PH, Matzuk MM. Functional microRNA involved in endometriosis. Mol Endocrinol 2011; 25:821–832.
45. Mutter GL, Zahrieh D, Liu C, Neuberg D, Finkelstein D, Baker HE, Warrington JA. Comparison of frozen and RNALater solid tissue storage methods for use in RNA expression microarrays. BMC Genomics 2004; 5: 88.
46. Su AI, Wiltshire T, Batalov S, Lapp H, Ching KA, Block D, Zhang J, Soden R, Hayakawa M, Kreiman G, Cooke MP, Walker JR, et al. A gene atlas of the mouse and human protein-encoding transcriptomes. Proc Natl Acad Sci U S A 2004; 101:6062–6067.
47. Talbi S, Hamilton AE, Vo KC, Tulac S, Overgaard MT, Dosiou C, Le Shay N, Nezhat CN, Kempson R, Lessey BA, Nayak NR, Giudice LC. Molecular phenotyping of human endometrium distinguishes menstrual cycle phases and underlying biological processes in normo-ovulatory women. Endocrinology 2006; 147:1097–1121.
48. Romundstad LB, Romundstad PR, Sunde A, von During V, Skjaerven R, Gunnell D, Vatten LJ. Effects of technology or maternal factors on perinatal outcome after assisted fertilisation: a population-based cohort study. Lancet 2008; 372:737–743.